tvst

Retina

Interobserver Agreement of Electrode to Retina Distance Measurements in a Second-Generation (44-Channel) Suprachoroidal Retinal Prosthesis

Carla J. Abbott[1,2], Elizabeth K. Baglin[1], Maria Kolic[1], Myra B. McGuinness[1,3], Samuel A. Titchener[4,5], Kiera A. Young[1], Jonathan Yeoh[1], Chi D. Luu[1,2], Lauren N. Ayton[1,2,6], Matthew A. Petoe[4,5], and Penelope J. Allen[1,2]

[1] Centre for Eye Research Australia, Royal Victorian Eye and Ear Hospital, Victoria, Australia
[2] Department of Surgery (Ophthalmology), University of Melbourne, Victoria, Australia
[3] Centre for Epidemiology and Biostatistics, Melbourne School of Population and Global Health, University of Melbourne, Victoria, Australia
[4] Bionics Institute of Australia, Victoria, Australia
[5] Medical Bionics Department, University of Melbourne, Victoria, Australia
[6] Department of Optometry and Vision Sciences, University of Melbourne, Australia

Purpose: The electrode to retina (ER) distance is an important contributory factor to the safety and efficacy of a suprachoroidal retinal prosthesis. Measuring ER distance may be performed by different observers during multisite studies. The aim of this study was to assess the interobserver agreement in measuring ER distance.

Methods: Three independent, trained observers measured ER distance from the center of each suprachoroidal electrode to the inner retinal pigment epithelium in spectral-domain optical coherence tomography (SD-OCT) B-scans. A total of 121 ER distance measurements from 77 B-scans collected over 5 months from one subject implanted with a second-generation 44-channel suprachoroidal retinal prosthesis (NCT03406416) were made by each observer.

Results: ER distance ranged from 208 to 509 µm. Pearson's correlation coefficient (ρ) showed agreement of 0.99 (95% confidence interval [CI] = 0.98–0.99) in measuring ER for each pairwise comparison. The mean difference in ER distance between observers ranged from 2.4 to 6.4 µm with pairwise limits of agreement (95% CI) of ±20 µm (5.5% of mean). Intraclass correlation coefficient (ICC) showed agreement of 0.98 (95% CI = 0.97–0.99) between observers.

Conclusions: There is high agreement in measuring ER distances for suprachoroidal retinal prostheses using our systematic approach between multiple, trained observers, supporting the use of a single observer for each image.

Translational Relevance: High interobserver agreement outcomes indicate that multiple, trained observers can be used to take ER measurements across different images in suprachoroidal retinal prosthesis studies. This improves multisite study efficiency and gives confidence in interpreting results relating to the safety and efficacy of suprachoroidal retinal prostheses.

Introduction

Retinal prostheses are medical devices designed to provide a form of artificial vision by stimulating residual retinal cells in people with photoreceptor degeneration. They have so far been used mainly in people with ultra-low vision from inherited retinal disease, such as retinitis pigmentosa. Retinitis pigmentosa is the leading cause of irreversible vision loss in the working age population,[1,2] resulting in both peripheral and central vision loss in the advanced stages.

Globally to-date, 3 retinal prostheses have obtained regulatory approval, with over 500 people implanted, and more devices are in various stages of development.[3,4] Retinal prostheses have been designed for the epiretinal, subretinal, and suprachoroidal positions,[3,5] and clinical trials show they improve a recipients' ability to localize objects, orientate, and navigate.[3,6–12] The artificial vision produced is seen by recipients as a series of flashing lights, known as phosphenes.[13]

An important monitoring tool for safety and efficacy outcomes in retinal prosthesis clinical trials is the position of the device, relative to the retina. Thus, one of the measurements used for safety monitoring purposes is the electrode to retina (ER) distance, measured with spectral domain optical coherence tomography (SD-OCT).[8,11,14–19] For suprachoroidal and subretinal arrays, an increase in ER distance over time can indicate migration of the array, development of significant fibrosis around the array, or potentially a stimulation-specific inflammatory response, whereas a decrease in ER distance over time can indicate an issue with the conformability of the array to the eye or with the electrode position within the array substrate.[14,15,20] For epiretinal arrays, an increase in ER distance can also indicate migration of the array, development of significant fibrosis, or an issue with conformability, whereas retinal thickness can be monitored to assess if the array is putting force on the retinal tissue itself.[16–18,21,22] Epiretinal arrays, such as the Argus II are tacked at one end, so it is common that the distal end has an increased ER distance than the tacked end.[22] ER distance for suprachoroidal arrays[8,11,14,15] is measured from the center of each electrode to the outer retina, whereas for epiretinal arrays,[16–18] it is measured from the bottom of the array substrate to the inner retina at the edge of each electrode, because the epiretinal array location blocks the SD-OCT image through to the underlying retina.

An increase in ER distance has a negative effect on efficacy outcomes and requires a greater stimulation current to be used to evoke a phosphene.[16,23–28] In our initial clinical trial with a suprachoroidal prototype retinal prosthesis held in 2012–14 (Clinicaltrials.gov NCT01603576), we found a gradual increase of the ER distance over a 2-year period, in all 3 subjects, likely due to a combination of fibrosis and stimulation-induced inflammatory response.[8] Large variation in ER distance between subjects in cross-sectional studies with an epiretinal prostheses have also been reported, due to the biological (eye shape) factors, surgical factors (positioning of array on retinal plane), and fibrotic capsule formation, rather than from stimulation-induced inflammation.[17,18] Hence, monitoring ER distance is important, particularly in epiretinal and suprachoroidal device trials. Subretinal device trials have assessed OCT retinal appearance for adverse events, but not specifically measured ER distance.[29]

Our second generation, 44-channel suprachoroidal retinal prosthesis was implanted in 4 subjects with advanced retinitis pigmentosa in 2018 for feasibility study of safety and efficacy (Clinicaltrials.gov NCT03406416).[11,12,19,30] The procedure to measure the ER distance for each electrode in each subject over many time points is manual and time-consuming,[8,14] and hence, multiple, trained observers have performed this task over the course of the trial. Therefore, it is critical to ascertain the interobserver agreement of ER distance measurements to ensure the strategic use of a single observer for measuring each image and different observers for measuring each time point is appropriate. During the clinical trial, we found a mean change of approximately 200 µm in ER distance corresponds to a reduction in impedance of approximately 2 kΩ.[19] This is important as it forms the basis for judging the clinical significance of the interobserver limits of agreement, with a change in ER distance of >200 µm needed for a noticeable change in impedance and perceptual threshold to occur.

Although high interobserver agreement for measurements of retinal and choroidal thicknesses have been shown using SD-OCT,[31–37] it is unknown if this extends to measurements relating to implanted retinal devices. Hence, the aim of this study was to determine the interobserver agreement of ER distance measurements to indicate confidence in the use of multiple observers performing this task during future multisite retinal device trials.

Methods

Subjects

One subject with retinitis pigmentosa (RP) enrolled in a second-generation, 44-channel suprachoroidal retinal prosthetic device clinical trial (ClinicalTrials.gov identifier: NCT03406416) was chosen for analysis of ER distance measures based on having good fixation (limited nystagmus), clear media (posterior intraocular lens implanted), and resulting high quality SD-OCT scans (ability to obtain high resolution mode scans). The device clinical trial was approved by the Human Research and Ethics Committee of the Royal Victorian Eye and Ear Hospital (#16/1266H). Informed consent was obtained prior to enrollment and procedures adhered to the tenets of the Declaration of Helsinki. The male subject (age 39 at implantation) had
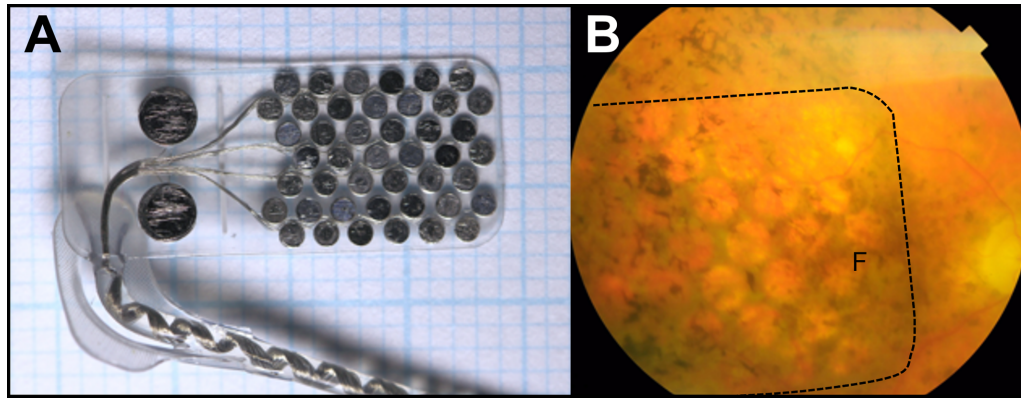
Figure 1. The second-generation, 44-channel, suprachoroidal retinal prosthesis. (**A**) Photograph of the retinal array showing the 44 stimulating platinum electrodes (Ø 1 mm) and 2 return platinum electrodes (Ø 2 mm) within a silicone substrate (19 × 8 mm). (**B**) Color fundus photograph showing the position of the array (*dotted lines*) implanted under the macula in the right eye of a subject with retinitis pigmentosa. Fovea = F.
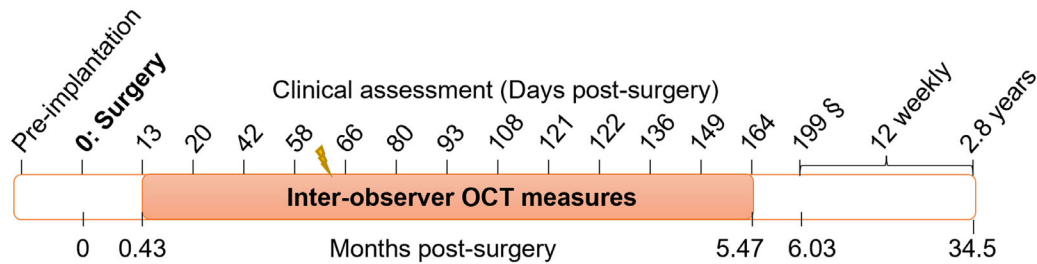

Figure 2. Timeline that interobserver SD-OCT measures were taken (*orange*) within the overall second-generation retinal prosthesis clinical trial for this subject (not to scale). SD-OCT measures were part of the suite of clinical assessments performed 2 to 4 weekly in the first 6 months after surgery, then at approximately 12 weekly intervals after the device fitting and training was complete (§), until the trial end point at 2.8 years postsurgery. Yellow lightning sign = device switch on (day 62 postsurgery).

end-stage RP (cone-rod dystrophy) with light perception vision in each eye and no islands of visual field remaining on the Goldmann perimetry. They reported legal blindness since age 13, and cessation of useful form vision since age 19. The remaining three subjects in the device clinical trial also had acceptable and comparable image quality, but due to the labor-intensive process of manual scan analysis by multiple observers, only one subject was selected for this study of the interobserver agreement of ER distance measures. The range of ER distance measures in the subject selected was known to be similar to the other three subjects.[19]

Retinal Prosthesis Implantation and Position

The subject was implanted with a second-generation, 44-channel, suprachoroidal retinal prosthesis in the right eye in February 2018, with surgical methods previously documented.[11,38] The electrode array consisted of 44 stimulating platinum electrodes (Ø = 1.0 mm) and 2 return platinum electrodes (Ø = 2.0 mm), on a silicone substrate (Fig. 1A).[11,14,19]

The surgical implantation was uncomplicated, with no device-related serious or unexpected adverse events reported.[11] The electrode array was positioned successfully according to the study protocol under the macula, as shown in Figure 1B.

SD-OCT Imaging

Following surgical implantation, retinal SD-OCT imaging (Spectralis; Heidelberg Engineering GmbH) was performed at regular time points to monitor the stability of the device and health of the implanted eye during the trial (Fig. 2). SD-OCT images used to determine the interobserver agreement of ER distance measurements were obtained over a 5-month period from 0.43 months to 5.47 months post-surgery (13 time points in total).

Single line B-scans were acquired through each electrode of the implanted array.[19] The infrared (IR) view was used to orientate the B-scan to align with the rows or columns of the electrode array (Fig. 3A). High resolution (HR) images were obtained where possible, but high speed (HS) images were captured at times
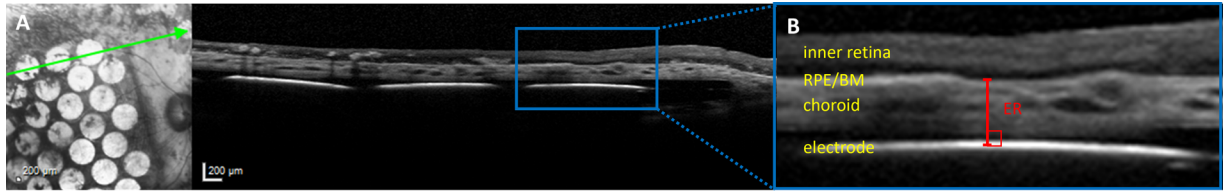
Figure 3. Electrode to retina (ER) distance measurement method. (**A**) IR image with green arrow indicating B-scan position aligned with the rows of the suprachoroidal electrode array. The accompanying SD-OCT B-scan image shows the position of the electrode array relative to the retina. (**B**) Magnified view of the region in the blue box in **A**, showing the inner retina, retinal pigment epithelium/Bruch's membrane (RPE/BM complex), choroid and suprachoroidal electrode, and the ER distance measurement (*red line*), measured perpendicularly from the center of the electrode to the inner RPE/BM complex.

due to poor fixation or strong eye movements (nystagmus). Overall, 82% (182 of 221) were taken at HR and 18% (39 of 221) were taken at HS. Automated real-time tracking (ART) averaging ranged from 1 to 51 B-scans. Images taken in HS mode with an ART of 1, or images in HR or HS modes with a quality score of less than 8, lacked the resolution required to visualize the boundary of the retinal pigment epithelium (RPE) or the electrode. Hence, for HS mode, a minimum ART of ≥ 2 was accepted, and for both modes, a minimum quality score of 8 was accepted. The axial resolution of B-scans in the Spectralis system is 3.9 μm (digital).[39]

Measurement of Electrode to Retina Distance

The ER distance associated with each electrode for each time point was measured by three trained, independent observers with measurements masked from each other (authors E.K.B. = observer 1, M.K. = observer 2, and S.A.T. = observer 3). All three observers had training in performing ER measurements according to the internal standard operating procedure[19] but had a variety of experience levels in performing OCT measurements. Two were qualified clinicians (orthoptists) with moderate clinical experience (observer 1; 7 years post-graduation) or extensive clinical experience (observer 2; 15 years post-graduation), and the third observer was a computer vision engineer (image processing) with recent experience in clinical psychophysics testing (observer 3; 2 years post-graduation).

ER distance was measured in microns from the center of the electrode to the inner boundary of the RPE/Bruch's membrane (BM) complex as shown in Figure 3B, following the procedure developed in our initial clinical trial and preclinical studies.[8,14] In end-stage RP, the RPE can often become difficult to identify separately from the BM. The observer first identified the center of an electrode by drawing a line along the middle plane of the electrode parallel with its surface. The ER distance in microns was measured perpendicularly to the electrode line, from the center of the electrode to the inner boundary of the RPE/BM. The electrodes were generally oriented parallel to the retina, but on rare occasions a small tilt was noted. Regardless of the presence of tilt, the ER distance was measured perpendicularly to the electrode face. Measurements were performed utilizing the mark-up tools within the Heidelberg Spectralis Heyex software and, for consistency, the scans were always viewed on the same screen, using the same magnification (200%), ratio (1:1), and contrast settings.

Statistical Analyses

Pearson's correlation coefficient (ρ) of ER distance was estimated for each pair of observers. The limits of agreement were estimated as the mean difference between each pair of observers plus or minus 1.96 times the standard deviation (95% interval for the mean difference).[40] The relationship between ER distance and agreement was visually assessed using Bland-Altman plots. Interobserver agreement was estimated using two-way random effects intraclass correlation (ICC) models for agreement. The ICC was then compared between subgroups defined by capture mode (HR versus HS), quality score (in quartile groupings), ART values (categorized as 1, 2, 3, or ≥ 4), and average ER distance (high versus low, dichotomized at median, 377 μm) via a z test to investigate factors that may be associated with interobserver agreement. Statistical analyses were conducted using Stata/SE version 16.1 (StataCorp, College Station, TX).

Results

ER Distance Measurements

A total of 121 ER measurements, from 77 B-scan images that met the quality and ART criteria were included. The ER distance measurements ranged from
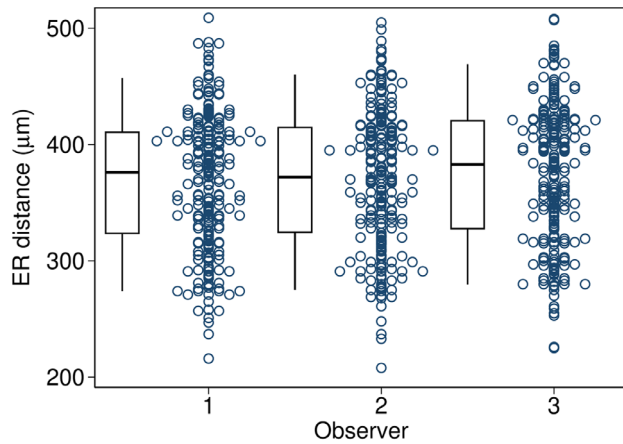
Figure 4. Distribution of electrode to retina (ER) measurements for each observer. On average, observer 1 had the shortest measurements (mean = 368 μm, range = 216–509 μm) and observer 3 had the longest (mean = 374 μm, range = 225–508 μm), with observer 2 (the most experienced observer) in between (mean = 370 μm, range = 208–505 μm). Each *circle* represents a single ER measurement; the *boxes* indicate the median and interquartile range with whiskers to the 5th and 95th centile for each observer.

208 to 509 μm across electrode positions and observers. This range is similar to the ER distance measures in the other three clinical trial subjects as measured by a single observer, and is mostly driven by eccentricity and degree of retinal degeneration.[19] The mean ER distance (±SD) measurements were 368 ± 59 μm for observer 1, 370 ± 60 μm for observer 2, and 374 ± 60 μm for observer 3 (Fig. 4). On average, observer 1 had the shortest measurements and observer 3 had the longest. Observer 2 with the most OCT measurement experience had mean ER distance measurements between the other 2 observers. The experience level of the observer did not overtly correlate with measurement length.

Pairwise Correlation

There was a high level of correlation between each pair of observers in measuring ER distance (Pearson's $\rho \geq 0.99$ for each pairwise comparison; Fig. 5). The mean difference in ER distance between observers
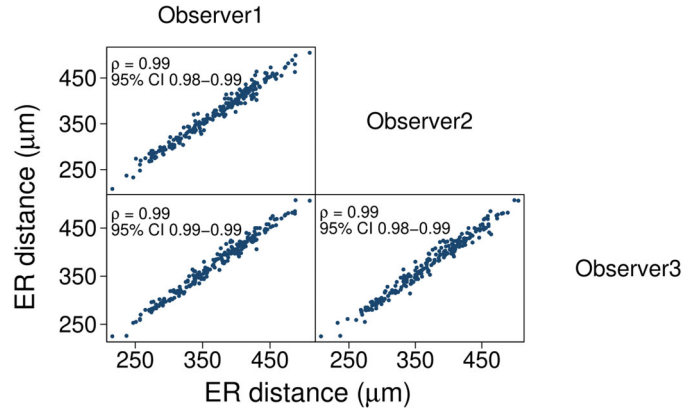

Figure 5. Scatter plot matrix showing a high level of agreement between each pair of observers. Pearson's $\rho \geq 0.99$ for each pairwise comparison.

ranged from 2.4 to 6.4 μm with 95% limits of agreement (±1.96 SD) on Bland-Altman plots for a specific image approximating ±20 μm (Table 1, Fig. 6). Hence, a change in ER distance of >20 μm would be considered as outside the normal measurement variation. The limits of agreement (±20 μm) correspond to 5.5% of the mean retinal thickness (approximately 370 μm), indicating a low measurement error. Furthermore, the interobserver limits of agreement are a factor of 10 below the change in ER distance (>200 μm)[19] needed for a noticeable change in impedance and perceptual threshold to occur and hence are clinically insignificant. There was no relationship between the difference between observers and the mean ER distance in the Bland-Altman plots (see Fig. 6).

Interobserver Agreement

The ICC for agreement was 0.98 (95% confidence interval [CI] = 0.98–0.99), showing very little variation between observers compared to the variation between images. ICC values between 0.81 and 1.0 are considered in statistical literature to be in "almost perfect" agreement.[41] Interobserver agreement was higher for images captured in HR mode than HS mode ($P < 0.001$) and for shorter ER distances ($P = 0.004$; Table 2),

Table 1. Pairwise Agreement in ER Distance Among Observers

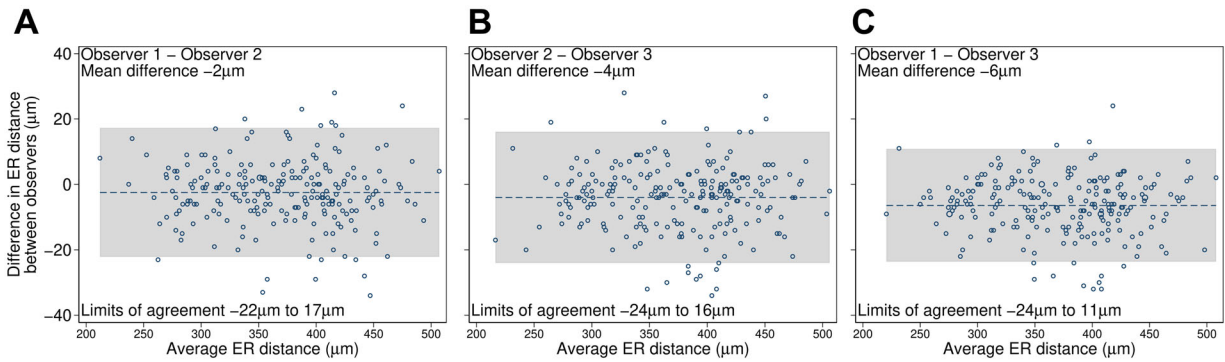|		Electrode to Retina Distance (μm)				
	Observer	Mean (SD)	Mean Difference (SD)	95% Limits of Agreement	Pearson's Correlation	(95% CI)
Agreement with observer 2	1	368.0 (59.1)	−2.4 (10.0)	±19.7 (−22.1, 17.3)	0.99	(0.98, 0.99)
	3	374.4 (59.8)	4.0 (10.2)	±20.1 (−16.1, 24.0)	0.99	(0.98, 0.99)
Agreement with observer 3	1	368.0 (59.1)	−6.4 (8.8)	±17.2 (−23.6, 10.8)	0.99	(0.99, 0.99)
	2	370.4 (59.7)	−4.0 (10.2)	±20.1 (−24.0, 16.1)	0.99	(0.98, 0.99)

Figure 6. Bland-Altman plots for electrode to retina (ER) distance for (A) Observer 1 versus 2, (B) Observer 2 versus 3, and (C) Observer 1 versus 3. The mean difference in ER distance between observers ranged from 2.4 to 6.4 µm with limits of agreement (±1.96 SD) shown in *grey*, representing the range of normal measurement variation relevant clinically. Each *circle* represents a single measurement location.

Table 2. Intraclass Correlation According to Image Characteristics

	Images	ICC	(95% CI)	*P* Value[*]
Mode				
High speed	39	0.94	(0.88, 0.97)	Reference
High resolution	182	0.99	(0.98, 0.99)	<0.001
Quality				
8 to 16	45	0.98	(0.96, 0.99)	Reference
17 to 20	47	0.99	(0.98, 0.99)	0.064
21 to 26	58	0.97	(0.95, 0.98)	0.469
27 to 36	71	0.99	(0.98, 0.99)	0.089
ART				
1	15	0.98	(0.96, 0.99)	Reference
2	98	0.98	(0.97, 0.99)	0.922
3	44	0.99	(0.98, 0.99)	0.611
4+	64	0.98	(0.97, 0.99)	0.558
Average ER distance				
≤377 µm	110	0.96	(0.94, 0.98)	Reference
>377 µm	111	0.92	(0.87, 0.95)	0.004

ART, automated real-time tracking; ER, electrode to retina; ICC, intraclass correlation coefficient for agreement.

[*]*P* value from z test.

however, the ICC for HS and long ER distances were still high at 0.94 and 0.92, respectively. No difference in ICC was observed when images were compared by quality or ART level. When specifically examining the instances of larger measurement differences (>20 µm) between observers for a single image in a case-by-case way, it was often related to differing judgments in the inner RPE boundary due to local variability of pigment clumping associated with the pathology of RP. An example in Figure 7, shows that observer 1 and observer 3 judged the center of the electrode to be in slightly different positions. Due to local RPE pigment clumping variations, this resulted in a difference in ER distance of 32 µm (observer 1 = 385 µm versus observer

2 = 417 µm). However, when examining cases specifically showing differences between HR and HS modes, such as the example in Figure 8, some of the greater discrepancy in HS mode may relate to the positioning of the measurement bar in the X direction relative to the choroidal features. Furthermore, in this example, due to differences in ART, the HR mode appears of reduced quality relative to the HS mode. This can also cause smoothing of the pigment clumping at the RPE boundary and hence reduce differences between observers in ER distance measurement. However, the data did not show an effect for either image quality or ART across the overall dataset.

Discussion

This study shows that manual measurements of ER distance using SD-OCT in patients with a suprachoroidal retinal prosthesis show high agreement between multiple trained observers (ICC) and high correlation between each pair of observers (Pearson's ρ). Interobserver agreement (ICC) was slightly higher for images captured in HR mode than HS mode, and for shorter ER distances than for longer ER distances. However, given the interobserver agreement was still high for HS mode and longer ER distances, the use of multiple observers is justified for both modes and for all ER distance measures. Furthermore, the point-by-point pairwise differences for observers, as shown across the ER distance in Bland-Altman plots, indicate there is no clinically relevant difference as a function of ER distance as there are not a higher number of datapoints outside the limits of agreement for longer ER distances across any of the observer pairs. There was no difference in ICC for different
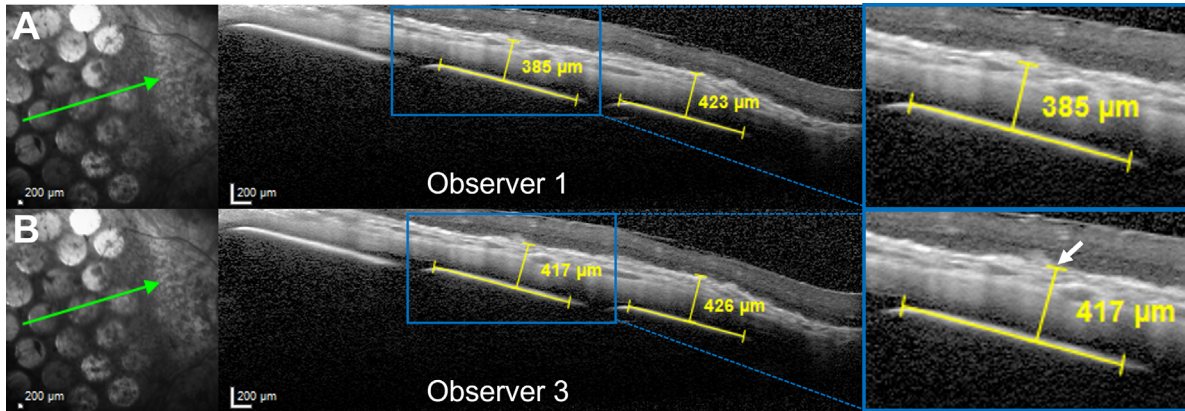
Figure 7. Example of ER distance measurement variation among observers related to pigment migration/clumping at the RPE. Infrared and accompanying SD-OCT B-scan images. The *green arrow* indicates the position of the B-scan in the infrared image. Measurement of the ER distance for 2 electrodes as marked by observer 1 (**A**) and observer 3 (**B**). *Blue box* regions show a magnified view of one ER measurement. The 32 µm difference in ER distance between observers in this example is due to a difference in identification of the center of the electrode and local variation in pigment clumping (*white arrow*) at the inner RPE boundary.
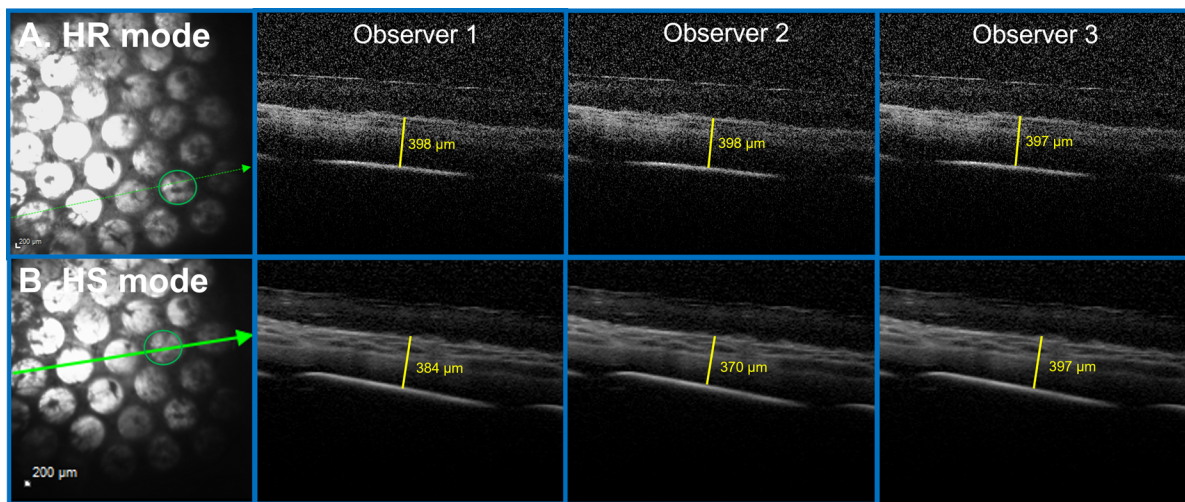

Figure 8. Representative comparison of ER distance measures between observers for HR mode compared to HS mode. (**A**) Infrared and OCT B-scan in HR mode (ART 3, image quality 32) for electrode #B6. (**B**) Infrared and OCT B-scan in HS mode (ART 40, image quality 34) for electrode #B4. The *green arrows* indicate B-scan position on the infrared image, the *green circles* indicate the electrode position measured for each example. The difference in ART between HR and HS mode likely explains the difference in apparent image quality. The agreement was higher between observers in HR mode, which may be due to differences in positioning of the ER distance measurement bar along the X axis, and/or reduced image quality causing smoothing of the RPE boundary line.

image quality or averaging (ART) parameters, however, given the inclusion of HR scans with an ART of 1, but not HS scans with an ART of 1, confounding may be occurring causing a mild distortion of the true relationship.[42]

Our results of high agreement between observers and high ICC are similar to SD-OCT studies of retinal and choroidal thickness measurements, where good interobserver agreement and only small differences between observers are found (ICC = 0.82–0.99).[31–37] Most of these studies used 2 observers with very high ICC (>0.90), however, a study using 9 independent observers still obtained an ICC of 0.82.[31] Our study used 3 independent observers, with an overall ICC of ≥0.98. Together, comparison with these previous studies using manual segmentation of choroidal and retinal structures suggests that studies using >2 observers are still highly reliable. Comparing with

studies measuring choroidal thickness are particularly useful because with a suprachoroidal prosthesis the measurement is from just outside the choroid (electrode position in suprachoroidal space) to the inner edge of the RPE, which incorporates the choroidal thickness itself.

High interobserver agreement occurred despite large variation in ER distance across the retina, with ER distance ranging from 208 to 509 μm across electrode positions and observers. The large range of ER distance was due to a combination of disease pathology (RPE clumping and variable choroidal thickness due to RP) and variation of ER distance over the array due to the biomechanics and conformability of the array in the suprachoroidal space.[14] Although the mean difference in ER distance between observers (2.4 to 6.4 μm) was clinically insignificant (less than the axial resolution of the Spectralis; 3.9 μm digital[39]) at <2% of the mean ER distance in this subject (approximately 370 μm), the limits of agreement between observers (±20 μm; 95% CIs on Bland-Altman graphs) was 5.5% of the mean ER distance. This indicates the measurement error is low relative to the mean ER distance. Examination of the specific measurements where there was a difference of >20 μm between observer pairs showed that commonly the source of difference in individual pairs resulted from local variations in the RPE (pigment clumping) due to the pathology of RP so that a small difference in location of the electrode center between observers resulted in a larger difference in ER distance if there was a pigment clump in that local area.

The secondary question to be considered when interpreting the limits of agreement in pairwise correlation is regarding the size of the ER distance change that might be clinically important for retinal prosthesis safety and efficacy studies. This is linked to the relationship among perceptual thresholds, ER distance, and impedance, as it is known from our prototype suprachoroidal clinical trial (NCT01603576) that perceptual thresholds can increase with ER distance.[8,23] Our initial report[11] from the second-generation (44-channel) suprachoroidal clinical trial shows that ER distance can vary widely between prosthesis users and that the effect on perceptual threshold is also dependent on a range of factors, including impedance, retinal eccentricity, and effects of fading (phosphene familiarization). The detailed relationship among perceptual thresholds, ER distance, and impedance has been specifically addressed in a separate paper for the second-generation suprachoroidal trial,[19] however, we note a mean change of approximately 200 μm in ER distance (approximately 50% of total ER distance) corresponds to a reduction in impedance of approxi-

mately 2 kΩ. Therefore, the measurement variability in the current study of ±20 μm or 5.5% of the total ER distance, is well within the limit for clinical impact on device efficacy (200 μm; 50%). In other words, a change in ER distance of 200 μm is required to cause an impact on impedance outcomes, so the interobserver limits of agreement for measuring ER distance are clinically insignificant. Hence, there is high confidence that any clinically relevant change over time will be detected in longitudinal studies of suprachoroidal arrays with multiple observers.

The strength of the study included using multiple observers (more than 2) as would often be the case in a multisite trial. Limitations include use of only one subject implanted with a retinal prosthesis, although there were a high total number of data points (121) evaluated across a wide retinal eccentricity, high quality and resolution SD-OCT images were obtained, and the subject was known to have similar ER distances to the other clinical trial subjects of variable ages (range = 47–66 years).[19] However, it is possible that the interobserver agreement may be worse with lower quality images as might occur in eyes with media opacities or significant nystagmus. The method shown here is only suitable for suprachoroidal arrays, where there is clear unobstructed SD-OCT imaging of the retinal layers, in contrast to epiretinal implants, where the device blocks the imaging light source. For epiretinal arrays, groups have developed methods of ER distance assessment using the edge of the electrode (instead of the center) if the substrate is transparent (i.e. Argus II array)[16] or using the array edges if the substrate is not transparent (i.e. diamond retinal prosthesis).[21] In the future, it may be possible to automate the ER distance measuring process with an algorithm, as the borders between the electrode and the inner RPE/Bruch's membrane complex are high contrast and well-defined, even in RP. This would make the safety monitoring of suprachoroidal prostheses faster and provide greater sampling across the array. Other future studies could be conducted to build on the interobserver reliability results from this study. First, the interobserver agreement could be determined using more than one subject, across multiple ages, and over a greater time period to give greater confidence in the data being able to extrapolate across a greater variety of circumstances. If greater variability was present, then ICC may be lower. Second, the intra-observer agreement could be calculated using the same observer to take multiple measurements using the same B-scan, to put the interobserver agreement results in greater context, although it is known the error is low relative to the mean (5.5%). Third, the interobserver agreement could be calculated with observers from other

institutions. We are unaware of other clinical studies with a suprachoroidal electrode array where electrode to retina distance has been captured and measured for direct comparison of interobserver results, however, certainly it would be interesting to compare interobserver agreement on our dataset with experts from other institutions in the future. This point can also be extended to number of trial sites and number of surgeons in a multisite trial. Finally, future work could assess a greater number of observers, the impact of observer experience on results and whether experience level generates bias in any direction.

The results of excellent interobserver agreement in measuring ER distance provides confidence in interpreting results relating to the safety and efficacy of suprachoroidal retinal prostheses, including interpreting safety data from the second-generation (44-channel) suprachoroidal retinal prosthesis trial.[11] Valid estimates of change in ER distance over time can be produced despite using different observers at each time point, and the interobserver variability is well-within the change in ER distance that would cause a clinically relevant change in impedance. Although OCT scan data from only one subject was analyzed, the measurement method appears robust and suggests that multiple trained observers can be used to perform ER distance measures during future multisite suprachoroidal retinal prosthesis trials, with minimal risk of interobserver measurement differences impacting on device safety and efficacy results.

References

1. Liew G, Michaelides M, Bunce C. A comparison of the causes of blindness certifications in England and Wales in working age adults (16–64 years), 1999–2000 with 2009–2010. *BMJ Open.* 2014;4:e004015.
2. Heath Jeffery RC, Mukhtar SA, McAllister IL, et al. Inherited retinal diseases are the most common cause of blindness in the working-age population in Australia. *Ophthalmic Genet.* 2021;42(4):431–439.
3. Ayton LN, Barnes N, Dagnelie G, et al. An update on retinal prostheses. *Clin Neurophysiol.* 2020;131:1383–1398.
4. Allen PJ. Retinal prostheses: Where to from here? *Clin Exp Ophthalmol.* 2021;49(5):418–429.
5. Cheng DL, Greenberg PB, Borton DA. Advances in retinal prosthetic research: a systematic review of engineering and clinical characteristics of current prosthetic initiatives. *Curr Eye Res.* 2017;42:334–347.
6. da Cruz L, Dorn JD, Humayun MS, et al. Five-year safety and performance results from the Argus II retinal prosthesis system clinical trial. *Ophthalmology.* 2016;123:2248–2254.
7. Stingl K, Bartz-Schmidt KU, Besch D, et al. Subretinal visual implant alpha IMS–clinical trial interim report. *Vis Res.* 2015;111:149–160.
8. Ayton LN, Blamey PJ, Guymer RH, et al. First-in-human trial of a novel suprachoroidal retinal prosthesis. *PLoS One.* 2014;9:e115239.
9. Edwards TL, Cottriall CL, Xue K, et al. Assessment of the electronic retinal implant alpha AMS in restoring vision to blind patients with end-stage retinitis pigmentosa. *Ophthalmology.* 2018;125:432–443.
10. Delyfer MN, Gaucher D, Mohand-Saïd S, et al. Improved performance and safety from Argus II retinal prosthesis post-approval study in France. *Acta Ophthalmol.* 2021;99(7):e1212–e1221.
11. Petoe MA, Titchener SA, Kolic M, et al. A second generation (44-channel) suprachoroidal retinal prosthesis: Interim clinical trial results. *Transl Vis Sci Technol.* 2021;10:12.
12. Karapanos L, Abbott CJ, Ayton LN, et al. Functional Vision in the Real-World Environment With a Second-Generation (44-Channel) Suprachoroidal Retinal Prosthesis. *Transl Vis Sci Technol.* 2021;10:7.
13. Sinclair NC, Shivdasani MN, Perera T, et al. The appearance of phosphenes elicited using a suprachoroidal retinal prosthesis. *Invest Ophthalmol Vis Sci.* 2016;57:4948–4961.

14. Abbott CJ, Nayagam DA, Luu CD, et al. Safety studies for a 44-channel suprachoroidal retinal prosthesis: a chronic passive study. *Invest Ophthalmol Vis Sci.* 2018;59:1410–1424.

15. Nayagam DA, Williams RA, Allen PJ, et al. Chronic electrical stimulation with a suprachoroidal retinal prosthesis: a preclinical safety and efficacy study. *PLoS One.* 2014;9:e97182.

16. de Balthasar C, Patel S, Roy A, et al. Factors affecting perceptual thresholds in epiretinal prostheses. *Invest Ophthalmol Vis Sci.* 2008;49:2303–2314.

17. Rizzo S, Cinelli L, Finocchio L, et al. Assessment of postoperative morphologic retinal changes by optical coherence tomography in recipients of an electronic retinal prosthesis implant. *JAMA Ophthalmol.* 2019;137:272–278.

18. Yoon YH, Humayun MS, Kim YJ. One-year anatomical and functional outcomes of the Argus II implantation in Korean patients with late-stage retinitis pigmentosa: A prospective case series study. *Ophthalmologica.* 2021;244:291–300.

19. Titchener SA, Nayagam DA, Kvansakul J, et al. A Second-Generation (44-Channel) Suprachoroidal Retinal Prosthesis: Long-Term Observation of the Electrode–Tissue Interface. *Transl Vis Sci.* 2022;11:12.

20. Butterwick A, Huie P, Jones B, et al. Effect of shape and coating of a subretinal prosthesis on its integration with the retina. *Exp Eye Res.* 2009;88:22–29.

21. Fox K, Meffin H, Burns O, et al. Development of a magnetic attachment method for bionic eye applications. *Artif Organs.* 2016;40:E12–E24.

22. Parmeggiani F, De Nadai K, Piovan A, et al. Optical coherence tomography imaging in the management of the Argus II retinal prosthesis system. *Eur J Ophthalmol.* 2017;27:e16–e21.

23. Shivdasani MN, Sinclair NC, Dimitrov PN, et al. Factors affecting perceptual thresholds in a suprachoroidal retinal prosthesis. *Invest Ophthalmol Vis Sci.* 2014;55:6467–6481.

24. Ahuja A, Yeoh J, Dorn J, et al. Factors affecting perceptual threshold in Argus II retinal prosthesis subjects. *Transl Vis Sci Technol.* 2013;2:1.

25. Naidu A, Ghani N, Yazdanie MS, et al. Effect of the electrode array-retina gap distance on visual function in patients with the Argus II retinal prosthesis. *BMC Ophthalmol.* 2020;20:1–8.

26. Xu LT, Rachitskaya AV, DeBenedictis MJ, et al. Correlation between Argus II array–retina distance and electrical thresholds of stimulation is improved by measuring the entire array. *Eur J Ophthalmol.* 2021;31:194–203.

27. Pham P, Roux S, Matonti F, et al. Post-implantation impedance spectroscopy of sub-retinal micro-electrode arrays, OCT imaging and numerical simulation: towards a more precise neuroprosthesis monitoring tool. *J Neural Eng.* 2013;10:046002.

28. Kasi H, Bertsch A, Guyomard J-L, et al. Simulations to study spatial extent of stimulation and effect of electrode–tissue gap in subretinal implants. *Med Eng Phys.* 2011;33:755–763.

29. Stingl K, Bach M, Bartz-Schmidt KU, et al. Safety and efficacy of subretinal visual implants in humans: methodological aspects. *Clin Exp Optom.* 2013;96:4–13.

30. Titchener SA, Kvansakul J, Shivdasani MN, et al. Oculomotor responses to dynamic stimuli in a 44-channel suprachoroidal retinal prosthesis. *Transl Vis Sci Technol.* 2020;9:31.

31. Esteban-Ortega M, Steiner M, García-Lozano I, et al. Reproducibility of manual choroidal thickness measurements using optical coherence tomography. *Arch Soc Esp Oftalmol.* 2020;95:379–385.

32. Chhablani J, Barteselli G, Wang H, et al. Repeatability and reproducibility of manual choroidal volume measurements using enhanced depth imaging optical coherence tomography. *Invest Ophthalmol Vis Sci.* 2012;53:2274–2280.

33. Spaide RF, Koizumi H, Pozzoni MC. Enhanced depth imaging spectral-domain optical coherence tomography. *Am J Ophthalmol.* 2008;146:496–500.

34. Branchini L, Regatieri CV, Flores-Moreno I, et al. Reproducibility of choroidal thickness measurements across three spectral domain optical coherence tomography systems. *Ophthalmology.* 2012;119:119–123.

35. Shao L, Xu L, Chen CX, et al. Reproducibility of subfoveal choroidal thickness measurements with enhanced depth imaging by spectral-domain optical coherence tomography. *Invest Ophthalmol Vis Sci.* 2013;54:230–233.

36. Flores-Rodríguez P, Gili P, Martín-Ríos MD. Sensitivity and specificity of time-domain and spectral-domain optical coherence tomography in differentiating optic nerve head drusen and optic disc oedema. *Ophthalmic Physiol Opt.* 2012;32:213–221.

37. Manjunath V, Taha M, Fujimoto JG, et al. Choroidal thickness in normal eyes measured using Cirrus HD optical coherence tomography. *Am J Ophthalmol.* 2010;150:325–329.e1.

38. Saunders AL, Williams CE, Heriot W, et al. Development of a surgical procedure for implantation of

a prototype suprachoroidal retinal prosthesis. *Clin Exp Ophthalmol.* 2014;42:665–674.

39. SPECTRALIS Diagnostic Imaging Platform from Heidelberg Engineering, Inc., https://www.optometryweb.com/6419-Optical-Coherence-Tomography-OCT-Equipment-Optical-Coherent-Tomography-Machines/3941784-SPECTRALIS-sup-reg-sup-HRA-OCT/. January 14, 2022.

40. Giavarina D. Understanding Bland Altman analysis. *Biochem Med (Zagreb).* 2015;25:141–151.

41. Landis JR, Koch GG. A one-way components of variance model for categorical data. *Biometrics.* 1977;33(4):671–679.

42. Skelly AC, Dettori JR, Brodt ED. Assessing bias: the importance of considering confounding. *Evid Based Spine Care J.* 2012;3:9–12.